Convex Combination for Source Localization Using Received Signal Strength Measurements

Qi Wang[1], Zhansheng Duan[1], X. Rong Li[2], Uwe D. Hanebeck[3]
[1] Center for Information Engineering Science Research, Xi'an Jiaotong University, Xi'an, Shaanxi 710049, China
[2]Department of Electrical Engineering, University of New Orleans, New Orleans, LA 70148, U.S.A
[3]Intelligent Sensor-Actuator-Systems Laboratory (ISAS), Institute for Anthropomatics and Robotics
Karlsruhe Institute of Technology (KIT), Germany
Email: chyk_wong@126.com, zsduan@mail.xjtu.edu.cn, xli@uno.edu, uwe.hanebeck@kit.edu

***Abstract*—Source localization is of great importance for wireless sensor network applications. Locating emission sources using received signal strength (RSS) measurements is investigated in this paper. As RSS localization is a non-convex optimization problem, it is difficult to achieve global optima. Many optimization methods have been proposed to relax it to a convex optimization problem. Unlike these methods, we propose a convex combination scheme. By introducing a highly accurate linear approximation of a logarithmic function, the source location is represented by a convex combination of a set of virtual anchors. Then the original problem is relaxed to be a convex optimization problem of finding the optimal combination coefficients, which can be solved efficiently using constrained least squares. To obtain the virtual nodes, we construct parallel lines and use their intersections to form a convex polygon, which covers the source location with certain probability. The vertices of the polygon are taken as the virtual nodes. Numerical examples verify the performance of the proposed method in both localization accuracy and computational efficiency.**

***Index Terms*—Received signal strength (RSS), Source localization, Convex combination, Virtual nodes**

I. Introduction

Wireless localization has gained much attention in recent years [1-2]. Most current localization techniques for wireless networks are based on measurements of different physical characteristics of a radio signal. These characteristics include time of arrival (TOA), time difference of arrival (TDOA), angle of arrival (AOA), and received signal strength (RSS) [3-5]. Among these, RSS-based localization has been widely used in many applications, such as emergency communications, public safety, and intelligent transportation [6-8]. It benefits from the easy availability of RSS measurements since many wireless devices can conveniently measure signal strength during normal communication, such as smart phones, laptops, and tablets. In addition, RSS measurements have a low cost [9-10].

To determine a stationary source position based on the RSS measurements is a parameter estimation problem. Many RSS localization methods have been proposed in the literature [11-17]. They include maximum likelihood (ML) and least-squares (LS) estimators. The ML estimator for the RSS model needs to deal with a non-convex problem. This is difficult because common iterative algorithms, such as gradient descent, can hardly obtain the globally optimal solution due to its sensitivity to initialization [18]. To tackle this problem, other approaches have been studied. The semidefinite programming (SDP) approach relaxes the original non-convex problem to a convex problem via semidefinite programming. By a special rearrangement, the linear LS method transforms the nonlinear RSS model into a linear model and then obtains the LS solution. In [15] and [16], two SDP and LS methods have been proposed for RSS localization with an unknown transmission power. For the SDP method, it transforms the nonconvex ML cost function to a convex one by using proper approximations and relaxations. It also linearizes the measurement model and applies the LS solution to the linearized model. Inspired by this, we have proposed SDP and constrained LS methods for RSS localization coupled with sensor registration [19]. As the constrained LS method exploits more information, it can provide better performance than the unconstrained LS method. Other RSS localization approaches have been studied as well, such as fingerprinting localization [14] and device-free localization [17]. The former first constructs an RSS fingerprint database in the training phase and then estimates the location by matching the user's reported fingerprints in the database in the localization phase. In the latter method, the target is not equipped with any electronic tag for communicating with the localization system. It estimates a target's location by fusing the changes in the RSS measurement of the wireless links.

Unlike the above methods, this work proposes a convex-combination based RSS-localization (CCRL) method for source localization. This convex combination idea was first proposed for the AOA localization [20]. We extend it to RSS localization. It differs from the geometric approach in AOA localization. Here, the position of the source is estimated in several steps: First, determine a convex hull that covers a small neighborhood of the source with a certain probability. Meanwhile, generate the vertices of the convex hull, named virtual nodes. Then represent the source position as a con-

Research supported in part by National Natural Science Foundation of China through grant 61673317 and 61673313, and the Fundamental Research Funds for the Central Universities of China.

vex combination of these coarse estimates, with non-negative combination coefficients that sum up to one. The RSS at each sensor can be regarded as the same combination of the ones emitted from the virtual nodes. This approximation is justified because its error is a higher-order infinitesimal than the radius of the minimum bounding ball of the convex hull. Thus, we have converted the nonlinear term in the optimization to a linear convex combination, so the optimization problem can be solved efficiently by a constrained LS method. In summary, the key to our CCRL method is to find the virtual nodes and compute the combination coefficients.

This paper is organized as follows. Section II introduces the RSS model and analyzes the disadvantage of the ML method. Section III presents the basic idea of convex combination based RSS localization. Section IV addresses the generation of the virtual nodes. In Section V, the performance of the proposed methods is demonstrated through numerical examples. Section VI concludes the paper.

II. Problem Formulation

Consider the RSS-based source localization in a wireless network of n sensors with coordinates $\mathbf{x}_i = \left[x_i, y_i\right]^T, i = 1, 2, ..., n$. Let $\mathbf{x}_s = \left[x_s, y_s\right]^T$ be the source location to be estimated. The RSS P_i (in dBm) at the ith sensor under the log-distance path loss and log-normal shadowing model is [21]

$$P_i = P_0 - 10\beta \log_{10} \frac{d_i}{d_0} + n_i, i = 1, 2, ..., n \tag{1}$$

where P_0 is a reference power at distance d_0 ($d_0 = 1m$ usually) from the source, $d_i = \|\mathbf{x}_s - \mathbf{x}_i\|_2$ is the distance between the source and the ith sensor, β is the path loss exponent, and the noise n_i's are (modeled as) independent and identically distributed zero-mean Gaussian random variables with variance σ^2.

Thus, the ML or LS estimator of the source position based on the measurements of the n sensors can be formulated as the following minimization problem

$$\hat{\mathbf{x}} = \arg\min_{\mathbf{x}_s} \sum_{i=1}^{n} \left\| P_i - \phi\left(\mathbf{x}_s, \mathbf{x}_i\right) \right\|^2 \tag{2}$$

where $\phi\left(\mathbf{x}_s, \mathbf{x}_i\right) = P_0 - 10\beta \log_{10} \frac{d_i}{d_0}$. It is generally hard to find the globally optimal solution due to the non-convexity of the objective function. This leads us to employing a suboptimal method, presented in detail next.

III. Convexification

Definition 1 *The convex hull of a given set $\mathbb{C}$ is the set of all convex combinations of points in $\mathbb{C}$* [22].

This leads to the following property. It can be illustrated easily.

Property 1 *Any point in a convex polygon can be represented as a combination of the vertices of the polygon.*

Suppose we can find a convex polygon that covers a small neighborhood around the actual source position. Let v_i be the location of the ith vertex and $\mathbf{V} = [v_1, v_2, .., v_m]$ be the matrix of the polygon vertices. We regard these vertices as virtual

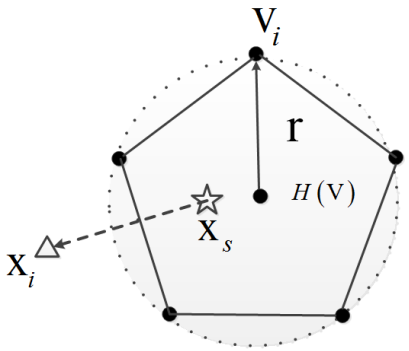

Fig. 1. Illustration of the approximation of RSS measurement

(source) nodes. Then, we can represent the location of the source by a linear combination of the virtual nodes

$$\mathbf{x}_s = \mathbf{V}\mathbf{w} \tag{3}$$

where $\mathbf{w} = [w_1, w_2, ..., w_m]^T, w_j \geq 0$ for all $j = 1, 2, ..., m$, and $\|\mathbf{w}\|_1 = \sum_{j=1}^{m} w_j = 1$. As such, we have converted the original optimization problem (2) to

$$\mathbf{w}^* = \arg\min_{\mathbf{w}} \sum_{i=1}^{n} \left\| P_i - \phi\left(\mathbf{V}\mathbf{w}, \mathbf{x}_i\right) \right\|^2, \text{ s.t. } \|\mathbf{w}\|_1 = 1, \mathbf{w} \geq \mathbf{0} \tag{4}$$

Notice that function $\phi(\cdot, \cdot)$ is nonlinear, which renders the optimization problem (4) nonconvex. However, we can approximate it by a linear form based on Theorem 1 next. The approximation accuracy can be guaranteed under some proper conditions.

Theorem 1 Given a set of points $\mathbf{S} = \{v_1, v_2, ..., v_m\} \subset \mathbf{R}^L$ (L-dimension real space) and $\mathbf{C} \subset \mathbf{R}^L$ a convex set covering $\mathbf{S}$. For an arbitrary point $\mathbf{x}_s \in \mathbf{C}$, define a point set $\mathbf{V}(\rho) \triangleq \{v_1(\rho), v_2(\rho), ..., v_m(\rho)\}$, where $v_k(\rho) = (1-\rho)\mathbf{x}_s + \rho v_k$ and $\rho \in [0, 1]$. Let $r(\rho)$ be the radius of the bounding ball $B(\mathbf{V}(\rho))$ of $\mathbf{V}(\rho)$, and $z_\infty \in \mathbf{R^L}$ be a point outside $\mathbf{C}$. Then for any finite integer $m \geq 2$ and all possible points $\mathbf{x}_s$ and z_∞ and points set $\mathbf{V}(\rho)$, we have

$$\lim_{\rho \to 0} \frac{\sum_{k=1}^{m} w_k \phi\left(v_k(\rho), z_\infty\right) - \phi\left(\sum_{k=1}^{m} w_k v_k(\rho), z_\infty\right)}{r(\rho)} = 0 \tag{5}$$

where $\sum_{k=1}^{m} w_k = 1, w_k \in [0, 1]$.

Proof: See Appendix.

Theorem 1 was inspired by [20]. From it, we have the following approximation

$$\phi\left(\mathbf{V}\mathbf{w}, \mathbf{x}_i\right) = \phi\left(\sum_{j=1}^{m} w_j v_j, \mathbf{x}_i\right) \approx \sum_{j=1}^{m} w_j \phi\left(v_j, \mathbf{x}_i\right) = \left(\Phi\mathbf{w}\right)_i \tag{6}$$

where $\Phi = \begin{bmatrix} \phi(v_1,\mathbf{x}_1) & \phi(v_2,\mathbf{x}_1) & \cdots & \phi(v_m,\mathbf{x}_1) \\ \phi(v_1,\mathbf{x}_2) & \phi(v_2,\mathbf{x}_2) & \cdots & \phi(v_m,\mathbf{x}_2) \\ \vdots & \vdots & \ddots & \vdots \\ \phi(v_1,\mathbf{x}_n) & \phi(v_2,\mathbf{x}_n) & \cdots & \phi(v_m,\mathbf{x}_n) \end{bmatrix}$,

$(\Phi\mathbf{w})_i$ is ith component of $\Phi\mathbf{w}$. When the radius of the bounding ball covering all the virtual nodes is sufficiently small, the above approximation accuracy can be guaranteed. That is, for an arbitrary anchor node, the signal strength it receives from the true source can be regarded as a convex combination of the ones it receives from the virtual nodes (see Fig. 1). The locations of the virtual nodes are known because they are generated by us but the combination coefficients are unknown. Thus, the original problem of estimating the source location is converted to a problem of estimating the coefficients. The error of this approximation, $\delta = \phi(\sum_{j=1}^{m} w_j v_j, \mathbf{x}_i) - \sum_{j=1}^{m} w_j \phi(v_j, \mathbf{x}_i)$, is a higher-order infinitesimal than $r(B(\mathbf{V}))$. This is the basis for our CCRL method.

According to Theorem 1, the non-convex optimization problem (2) can be approximated as the following constrained LS problem

$$\mathbf{w}^* = \arg\min_{\mathbf{w}} \|\mathbf{P} - \Phi\mathbf{w}\|^2, \text{ s.t. } \|\mathbf{w}\|_1 = 1, \mathbf{w} \geq \mathbf{0} \quad (7)$$

where $\mathbf{P} = [P_1, P_2, ..., P_n]^T$.

This new optimization problem can be solved easily. Once we obtain the optimal convex combination coefficients $\mathbf{w}^*$, the location of the source can be estimated as

$$\hat{\mathbf{x}} = \mathbf{V}\mathbf{w}^* \quad (8)$$

So far we have introduced the basic idea of our CCRL method. But there is one more problem to be solved, i.e., the generation of the virtual nodes.

IV. Virtual nodes generation

Next we introduce the generation scheme of the virtual nodes. We want to find some points that can form a convex hull covering the source location with a high probability. For each sensor, it can determine a ring-shaped subregion according to its measurement

$$r_i = \{(x,y) \,|\, |P_0 - P_i - 10\beta \log_{10} d_i(x,y)| \leq \alpha\sigma\} \quad (9)$$

That is,

$$10^{\frac{P_0 - P_i - \alpha\sigma}{5\beta}} \leq (x_i - x)^2 + (y_i - y)^2 \leq 10^{\frac{P_0 - P_i + \alpha\sigma}{5\beta}} \quad (10)$$

where $d_i(x,y) = \sqrt{(x_i - x)^2 + (y_i - y)^2}$, α is a parameter controlling the width of the ring. For a larger α, the ring will cover the source with a higher probability but the ring also becomes wider, which is not desirable since a narrower ring makes the approximation more accurate by Theorem 1. As each sensor can generate a ring from its measurement, the true source is located within the possible region $\mathcal{R}$ with probability

$$P((x,y) \in \mathcal{R} | \alpha, \sigma) = \prod_{i=1}^{n} P((x,y) \in r_i) = \prod_{i=1}^{n} p_i(\alpha) \quad (11)$$

where $\mathcal{R} = \cap_{i=1}^{n} r_i$ is the intersection of all rings and the noise is assumed to be i.i.d. Gaussian.

However, the intersection of rings is an irregular region, which is not necessarily convex. To deal with this problem, we generate a convex region that covers the intersection of the rings. That is, the convex region covers the source with a probability that is not less than that of the original one.

Suppose N rings produce an interset. The intersection is certainly a common region of each pair of rings. To find the convex region, we construct parallel lines for each pair of rings such that the intersection of the rings is sandwiched between the lines. By this, all parallel lines intersect the desired convex region. However, for N sensors, there are $C_N^2 \left(C_m^n = \frac{m!}{n!(m-n)!}\right)$ possible pairs of the parallel lines. Obviously, it is complex to obtain the parallel lines for every ring pair. To simplify the problem, we choose a reference sensor node j according to (12) since a smaller width of the ring indicates smaller noise involved. As a result, it reduces the number of parallel lines to $N - 1$. The computational complexity is then greatly reduced by using

$$j = \arg\min_i \tilde{r}_i, i = 1, 2, ..., N \quad (12)$$

where $\tilde{r}_i$ is the width of the ring r_i.

Once the reference sensor is determined, the parallel lines are generated for the reference ring (sensor) with other rings. Their intersections will form a convex region if there is only one region for the intersection. However, the parallel lines may produce multiple polygon intersections. It indicates that some lines are generated with large measurement error. Suppose all parallel lines intersect and produce K polygon intersections $\mathcal{P}_i, i = 1, 2, ..., K$. Let $\mathcal{P}_i$ have q_i pairs of lines. We find the polygon $\mathcal{P}_{i^*}$ by

$$i^* = \arg\max_i q_i, i = 1, 2, ..., K \quad (13)$$

That is, we discard the polygons formed by fewer parallel lines because they are more likely to correspond to larger measurement errors. Then, the vertices of $\mathcal{P}_{i^*}$ are regarded as the virtual nodes. Fig. 2 illustrates generation of the virtual nodes.

Next, we introduce the construction of the parallel lines. Consider two rings, we can find two parallel lines so that the intersection of the two rings is between the lines. Obviously, it has four cases, as in Fig. 3.

For case (a), the two lines connecting the points, as the intersections of the inner circle of one ring and the outer circle of the other ring, are parallel. The intersection of the two rings are between the parallel lines. However, cases (b), (c), and (d) are different: Case (b) has one intersection region; case (c) has no intersections, which may be caused by large noise. However, these two cases have the same relationship in terms of inner circle and outer circle (see Fig. 4(b)). Thus we can unify the construction of parallel lines for cases (b) and (c). Case (d) has no intersection either. However, the larger ring contains the other ring. In view of all these cases, we propose a scheme based on the distance relationship, where we consider

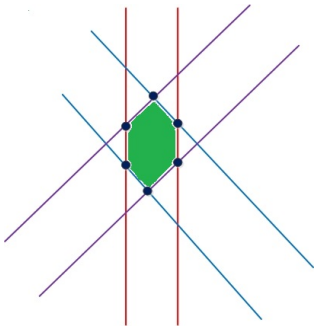

Fig. 2. Virtual nodes generation using the intersections of parallel lines

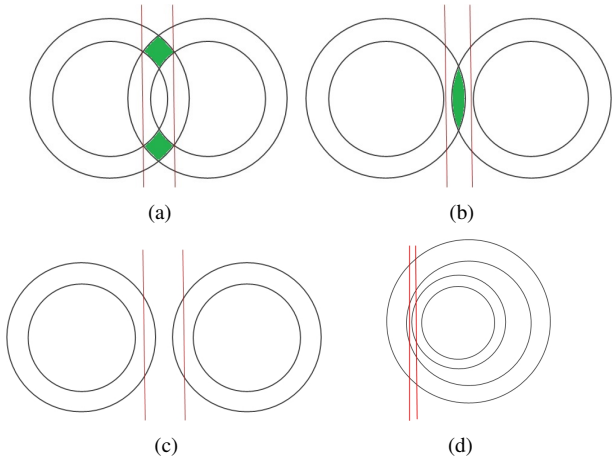

Fig. 3. Four cases for the location relationship of two rings

only the inner circle of one ring and the outer circle of the other ring. They are constituted based on the relative positions of the two circles (see Fig. 4):

Case I. If two circles have two intersection points, just connect the two points to generate the line (see Fig. 4(a)).

Case II. If they have no intersection points, we generate a line that is perpendicular to the line connecting the centers of the two circles and satisfies (see Figs. 4(b) and (c)):

$$AB/BC = r/R \tag{14}$$

In summary, Fig. 4(a) is for case (a), Fig. 4(b) is for cases (b) and (c), and Fig. 4(c) is for case (d).

The above are the basic idea and a complete procedure for generating virtual nodes. The CCRL algorithm can now be summarized:

(1) Choose a reference sensor node and generate the parallel lines to get the virtual nodes $\mathbf{V} = [v_1, v_2, .., v_m]$.

(2) Calculate $\phi_{i,j} = \phi(v_j, \mathbf{x}_i)$ and let

$$\Phi = \begin{bmatrix} \phi_{1,1} & \phi_{1,2} & \cdots & \phi_{1,m} \\ \phi_{2,1} & \phi_{2,2} & \cdots & \phi_{2,m} \\ \vdots & \vdots & \ddots & \vdots \\ \phi_{n,1} & \phi_{n,2} & \cdots & \phi_{n,m} \end{bmatrix}$$

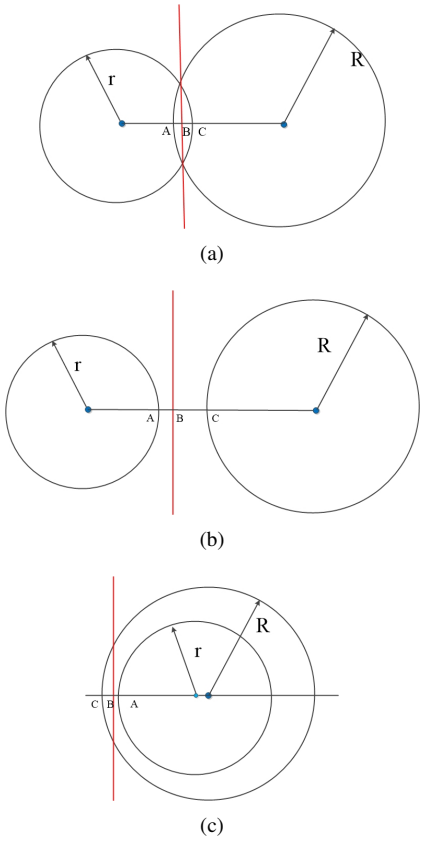

Fig. 4. Three cases for single line construction

(3) Calculate the optimal convex combination coefficient $\mathbf{w} = [w_1, w_2, ..., w_m]^T$ by the constrained LS:

$$\mathbf{w}^* = \arg\min_{\mathbf{w}} \sum_{i=1}^{n} \|P_i - \phi(\mathbf{V}\mathbf{w}, \mathbf{x}_i)\|^2, \text{ s.t. } \|\mathbf{w}\|_1 = 1, \mathbf{w} \geq \mathbf{0}$$

(4) Obtain the final estimate of the source location as

$$\hat{\mathbf{x}} = \sum_{j=1}^{m} w_j v_j$$

V. Illustrative Example

This section provides some illustrative examples to demonstrate the performance of the CCRL method. We consider two scenarios: a rectangular case and a circular case. We compare the performance of the CCRL method with the SDP method, the CLS method [19], the ML method and the CRLB, where ML is implemented numerically and initialized with the truth, which is unrealistic. The path loss exponent β and the reference power P_0 are set to 3 and -40 [23], respectively. The estimation performance is evaluated using the root-mean-square error (RMSE), averaged over 500 Monte Carlo runs.

A. RMSE versus noise deviation in rectangular case

In this scenario, 12 sensors are employed in the wireless network. They form a rectangle and the source is located inside or outside the rectangle. The noise standard deviation

varies from 1 to 20. We set $\alpha = 4$ (indicating a 4σ region) to ensure that the probability of each ring covering the source satisfies $\mathbf{P}(\mathbf{x}_s \in r_i) \geq 99.9\%$. We can see from Fig. 5 that the proposed method (CCRL) performs close to SDP and CLS methods (referred to the constrained LS methods) in Fig. 5. In Fig. 6, the proposed method performs better for almost all tested standard deviations. Fig. 7, however, shows that the CCRL method does not perform as well as other methods. Overall, the ML method performs best in all cases. However, if the ML method is initialized with a random value, it may have a poor performance since it is likely to achieve a local optimum instead of the global optimum.

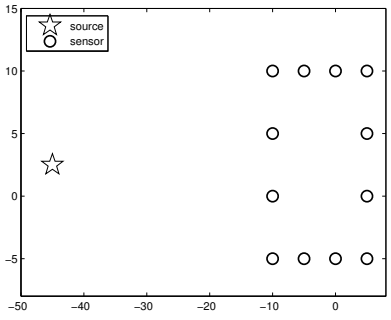

(a) Scenario

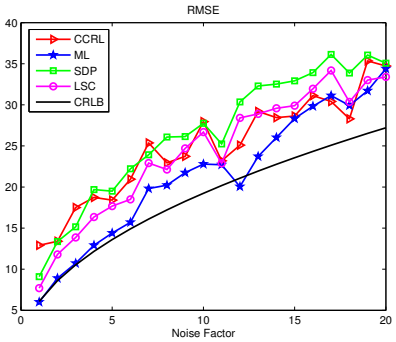

(b) RMSE of source localization

Fig. 5. The RMSE versus standard deviation of noise

B. RMSE versus noise deviation in circular case

In this scenario, 12 sensors form a circle. Other parameters are the same as in the rectangular case. Figs. 8, 9, and 10 show similar results as in the rectangular case. Note that our proposed method performs relatively better when the source is close to the boundary of the circle. When the source is far from the sensors or moves to the center of the circle, the relative performance of our CCRL method becomes worse gradually. This can be seen in both the rectangular case and the circular case, indicating that the relative performance of our CCRL method is scenario dependent. Actually, when the source is located at the centers of the rectangle and of the circle in Fig. 7 and Fig. 10, there will be more than one sensor which has a similar (short) distance to the source and receives similar

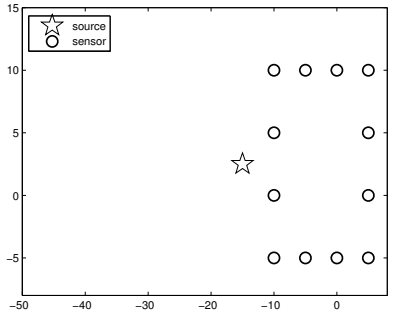

(a) Scenario

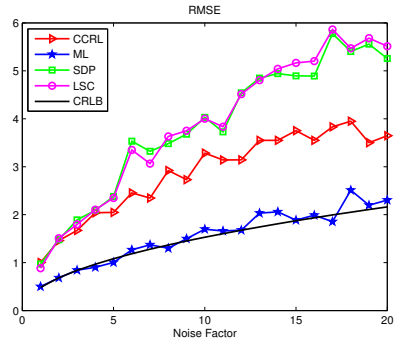

(b) RMSE of source localization

Fig. 6. The RMSE versus standard deviation of noise

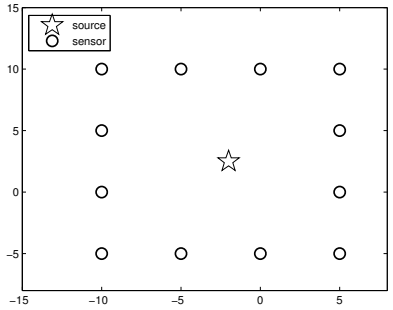

(a) Scenario

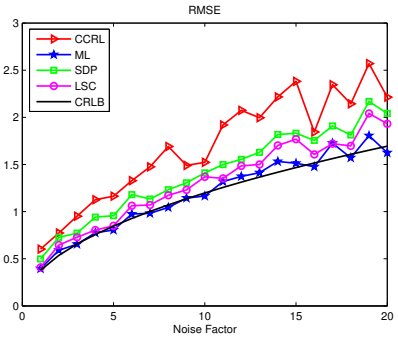

(b) RMSE of source localization

Fig. 7. The RMSE versus standard deviation of noise

RSS measurements. As a result of this, some uncertainty on choosing the reference sensor node will arise. Then, different reference sensors may be picked in the same scene for different Monte Carlo runs.

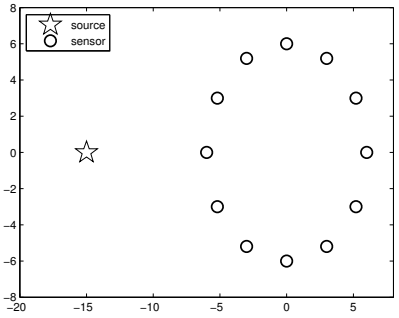

(a) Scenario

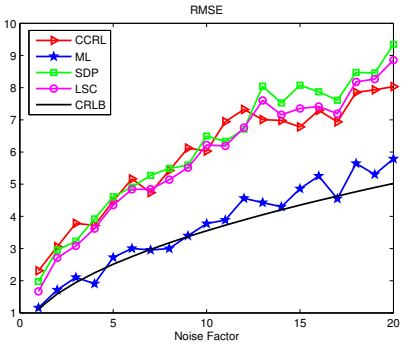

(b) RMSE of source localization

Fig. 8. The RMSE versus standard deviation of noise

C. RMSE versus α

The RMSEs of the proposed method versus α in both scenarios are illustrated in Fig. 11. The standard deviation of the noise is fixed as 2 and other parameters are the same as in Fig. 6 and Fig. 9. Generally, the localization RMSE becomes larger as α increases probably because a larger α results in a larger ring intersection. Although it may produce a convex region with a higher probability covering the source, a smaller convex region is strongly desired. In addition, for a Gaussian distributed random variable $x \sim \mathcal{N}(\overline{x}, \sigma)$, we have

$$P\{|x-\overline{x}|<\sigma\}=0.683 \quad P\{|x-\overline{x}|<2\sigma\}=0.954$$
$$P\{|x-\overline{x}|<3\sigma\}=0.997 \quad P\{|x-\overline{x}|<4\sigma\}=0.9997 \tag{15}$$

So if our requirement on the probability is not very high, a smaller α is preferred because a smaller convex region will be generated. Generally, α between 2 and 4 is preferred according to the experiment result.

D. Computational efficiency

To verify the computational efficiency of the proposed method, we compare the relative running time of the methods

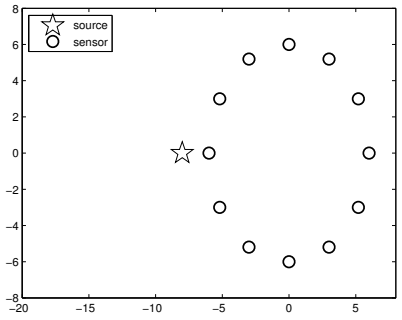

(a) Scenario

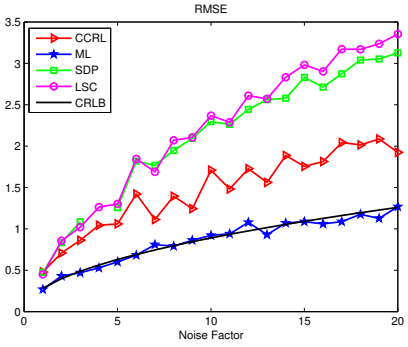

(b) RMSE of source localization

Fig. 9. The RMSE versus standard deviation of noise

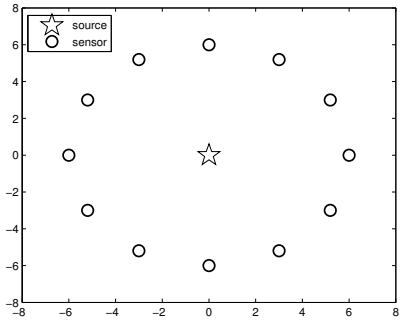

(a) Scenario

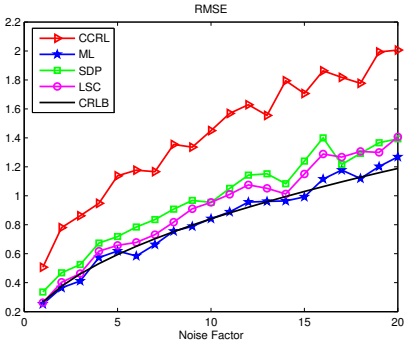

(b) RMSE of source localization

Fig. 10. The RMSE versus standard deviation of noise

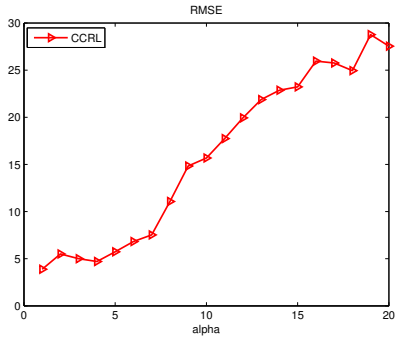

(a) Rectangular case

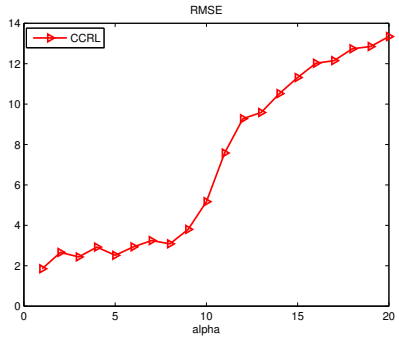

(b) Circular case

Fig. 11. The RMSE of localization versus α

considered, average over 500 Monte Carlo runs. The results are all relative to the CCRL method and given in Table I. It can be seen that our CCRL method is computationally more efficient than the others. Here, ML is not included as it depends on the initialization heavily.

Table I: Average Running Time

Algorithm	CCRL	SDP	LSC
Running time	1	1.438	1.417

VI. Conclusion

In this paper, we have proposed a convex combination based method for source localization. The estimate of the source location can be represented by a convex combination of virtual nodes. The transformed problem, a constrained LS problem, can be solved easily since it is convex. In the generation of the virtual nodes, the polygon formed by most parallel lines is used so that fewer measurements errors would be involved. By selecting a reference sensor, the computational complexity of generating parallel lines is greatly reduced. In numerical examples, we considered both rectangular and circular cases and showed that the proposed method has scenario dependent performance (relative to other methods) and provides a higher localization accuracy than our previous methods in some cases. Also note that a larger α (a parameter controlling probability) results in a larger RMSE in general. So a smaller α is preferred when the resulting convex region could cover the source with a satisfactory probability. In addition, our CCRL method is computationally more efficient than other methods.

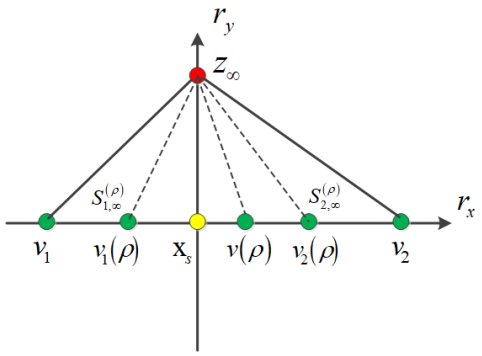

Fig. 12. Two-point case

Appendix

We use mathematical induction. First, consider the two-point case (i.e., $m = 2$, see Fig. 12).

Suppose that the 2-D plane is spanned by unit vectors r_x and r_y. Let $\mathbf{x}_s$ be at the origin. $v_1 = -R_1 r_x, v_2 = R_2 r_x$, R_1 and R_2 are scalars. $v_j(\rho) = (1-\rho)\,\mathbf{x}_s + \rho v_j$. Thus, $\mathbf{x}_s$ is in the hull of $\mathbf{V}(\rho)$. The radius of the bounding ball of $\mathbf{V}(\rho)$ is $r(\rho) = \rho(R_1 + R_2)/2$. Let $v(\rho) = \lambda v_1(\rho) + (1-\lambda) v_2(\rho)$. We can see that the hull shrinks to $\mathbf{x}_s$ as $\rho \to 0$. $z_\infty = h_x r_x + h_y r_y = (h_x, h_y)$.

Let $S_{j,\infty}^{(\rho)} = S(v_j(\rho), z_\infty)$ and

$$S(v_1(\rho), z_\infty) = P_0 - 10\beta \log_{10}\left(\sqrt{h_y^2 + (h_x + \rho R_1)^2}\right)$$

$$S(v_2(\rho), z_\infty) = P_0 - 10\beta \log_{10}\left(\sqrt{h_y^2 + (h_x - \rho R_2)^2}\right)$$

$$S(v(\rho), z_\infty) = P_0 - 10\beta \log_{10}\left(\sqrt{h_y^2 + (h_x - \rho R_2 + \lambda\rho(R_1 + R_2))^2}\right)$$

Clearly,

$$\lim_{\rho\to 0} \lambda S(v_1(\rho), z_\infty) + (1-\lambda) S(v_2(\rho), z_\infty) - S(v(\rho), z_\infty) = 0$$

and $\lim_{\rho\to 0} r(\rho) = 0$. Then, we have

$$\begin{aligned}
&\lim_{\rho\to 0} \frac{\lambda S(v_1(\rho),z_\infty)+(1-\lambda)S(v_2(\rho),z_\infty)-S(v(\rho),z_\infty)}{r(\rho)} \\
&= \lim_{\rho\to 0} \frac{\frac{\partial}{\partial\rho}[\lambda S(v_1(\rho),z_\infty)+(1-\lambda)S(v_2(\rho),z_\infty)-S(v(\rho),z_\infty)]}{\frac{\partial(r(\rho))}{\partial\rho}} \\
&= \frac{\left[\frac{-10\lambda\beta}{\ln 10}\frac{R_1 h_x}{h_x^2+h_y^2} + \frac{10(1-\lambda)\beta}{\ln 10}\frac{R_2 h_x}{h_x^2+h_y^2} + \frac{10\beta}{\ln 10}\frac{h_x(-R_2+\lambda R_1+\lambda R_2)}{h_x^2+h_y^2}\right]}{\frac{R_1+R_2}{2}} \\
&= 0
\end{aligned} \tag{16}$$

Thus Theorem 1 holds for the two-point case. Next consider the multiple-point case.

Suppose Theorem 1 holds for $m = t \geq 2$, that is,

$$\lim_{\rho\to 0} \frac{\sum_{j=1}^{t} \lambda_j S_{j,\infty}^{(\rho)} - S(z_\infty, \sum_{j=1}^{t} \lambda_j v_j(\rho))}{r(\rho)} = 0$$

For $m = t+1$, we constitute a new point

$$\tilde{v}_1 = \sum\nolimits_{j=2}^{t+1} \lambda'_j v_j(\rho)$$

where $\lambda'_j = \frac{\lambda_j}{1-\lambda_1} = \frac{\lambda_j}{\tilde{\lambda}_1}$.

Obviously, $\sum_{j=2}^{t+1} \lambda'_j = \frac{1}{1-\lambda_1} \sum_{j=2}^{t+1} \lambda_j = 1$. Thus we have

$$\lim_{\rho \to 0} \frac{\sum_{j=2}^{t+1} \lambda'_j S_{j,\infty}^{(\rho)} - S(z_\infty, \sum_{j=2}^{t+1} \lambda'_j v_j(\rho))}{r'(\rho)} = 0$$

where $r'(\rho)$ is the minimum radius of $H\left(\{v_2(\rho), ..., v_{t+1}(\rho)\}\right)$ (the hull composed by $v_2(\rho), v_3(\rho), ..., v_{t+1}(\rho)$).

It is not hard to see that $v_2(\rho), v_3(\rho), ..., v_{t+1}(\rho)$ all converge to $\mathbf{x}_s$ as $\rho \to 0$. Thus, $r'(\rho)$ and $r(\rho)$ are infinitesimal of the same order ($\rho \to 0$). Then we have

$$\lim_{\rho \to 0} \frac{\sum_{j=2}^{t+1} \lambda'_j S_{j,\infty}^{(\rho)} - S(z_\infty, \sum_{j=2}^{t+1} \lambda'_j v_j(\rho))}{r(\rho)} = 0$$

That is,

$$\sum\nolimits_{j=2}^{t+1} \lambda'_j S_{j,\infty}^{(\rho)} = S(z_\infty, \sum\nolimits_{j=2}^{t+1} \lambda'_j v_j(\rho)) + o\left[r(\rho)\right]$$

where $o\left[r(\rho)\right]$ represents a high-order infinitesimal than $r(\rho)$.

Then we have

$$\begin{aligned}
&\textstyle\sum_{j=1}^{t+1} \lambda_j S_{j,\infty}^{(\rho)} = \lambda_1 S_{1,\infty}^{(\rho)} + \sum_{j=2}^{t+1} \lambda_j S_{j,\infty}^{(\rho)} \\
=&\lambda_1 S_{1,\infty}^{(\rho)} + \textstyle\sum_{j=2}^{t+1} \tilde{\lambda}_1 \lambda'_j S_{j,\infty}^{(\rho)} \\
=&\lambda_1 S_{1,\infty}^{(\rho)} + \tilde{\lambda}_1 S\left(z_\infty, \textstyle\sum_{j=2}^{t+1} \lambda'_j v_j(\rho)\right) + \tilde{\lambda}_1 o\left[r(\rho)\right] \\
=&\lambda_1 S_{1,\infty}^{(\rho)} + \tilde{\lambda}_1 S\left(z_\infty, \tilde{v}_1\right) + \tilde{\lambda}_1 o\left[r(\rho)\right]
\end{aligned}$$

From the above, it follows that

$$\begin{aligned}
&\lim_{\rho \to 0} \tfrac{\sum_{j=1}^{t+1} \lambda_j S_{j,\infty}^{(\rho)} - S(z_\infty, \sum_{j=1}^{t+1} \lambda_j v_j(\rho))}{r(\rho)} \\
&= \lim_{\rho \to 0} \tfrac{\lambda_1 S_{1,\infty}^{(\rho)} + \tilde{\lambda}_1 S(z_\infty, \tilde{v}_1) + \tilde{\lambda}_1 o[r(\rho)] - S(z_\infty, \lambda_1 v_1(\rho) + \sum_{j=2}^{t+1} \lambda_j v_j(\rho))}{r(\rho)} \\
&= \lim_{\rho \to 0} \tfrac{\lambda_1 S_{1,\infty}^{(\rho)} + \tilde{\lambda}_1 S(z_\infty, \tilde{v}_1) - S(z_\infty, \lambda_1 v_1(\rho) + \tilde{\lambda}_1 \sum_{j=2}^{t+1} \lambda'_j v_j(\rho))}{r(\rho)} \\
&\qquad + \tfrac{\tilde{\lambda}_1 o[r(\rho)]}{r(\rho)} \\
&= \lim_{\rho \to 0} \tfrac{\lambda_1 S_{1,\infty}^{(\rho)} + (1-\lambda_1) S(z_\infty, \tilde{v}_1) - S(z_\infty, \lambda_1 v_1(\rho) + (1-\lambda_1) \tilde{v}_1)}{r(\rho)} \\
&\qquad + \tfrac{\tilde{\lambda}_1 o[r(\rho)]}{r(\rho)} \\
&= \lim_{\rho \to 0} \tfrac{\lambda_1 S(z_\infty, v_1(\rho)) + (1-\lambda_1) S(z_\infty, \tilde{v}_1) - S(z_\infty, \lambda_1 v_1(\rho) + (1-\lambda_1) \tilde{v}_1)}{r(\rho)} \\
&\qquad + \tfrac{\tilde{\lambda}_1 o[r(\rho)]}{r(\rho)} \qquad \text{(two-point case for } v_1(\rho) \text{ and } \tilde{v}_1) \\
&= 0
\end{aligned}$$

Thus Theorem 1 holds for all finite numbers m. This completes the proof.

REFERENCES

[1] A. Yassin, Y. Nasser, M. Awad, A. Al-Dubai, R. Liu, C. Yuen, R. Raulefs, and E. Aboutanios, "Recent advance in indoor localization: a survey on theoretical approaches and applications," *IEEE Communications Survey & Tutorials*, vol. 19, no. 2, pp. 1327-1346, Second Quarter 2017.

[2] S. Tomic, M. Beko, and R. Dinis, "3-D target localization in wireless sensor networks using RSS and AoA measurements," *IEEE Transactions on Vehicular Technology*, vol. 66, no. 4, pp. 3197-3210, Apr. 2017.

[3] S. Venkatraman and J. Caffery, "Hybrid TOA/AOA techniques for mobile location in non-line-of-sight environments," in *Proceedings of 2004 Wireless Communications and Networking Conference*, Atlanta, USA, March 2004, pp. 274-278.

[4] D. C. Popescu and M. Hedley, "Range data correction for improved localization," *IEEE Wireless Communication Letters*, vol. 4, no. 3, pp. 297-300, Jun. 2015.

[5] M. Z. Win, A. Conti, S. Mazuelas, Y. Shen, W. M. Gifford, D. Dardari, M. Chiani "Network localization and navigation via cooperation," *IEEE Communications Magazine*, vol. 49, no. 5, pp. 56-62, May. 2011.

[6] I. F. Akyildiz, W. Su, Y. Sankarasubramaniam, and E. Cayirci, "A survey on sensor networks," *IEEE Communications Magazine*, vol. 40, no. 8, pp. 102-114, Aug. 2002.

[7] P. Biswas, T.-C. Liang, K.-C. Toh, Y. Ye and T.-C. Wang, "Semidefinite programming approaches for sensor network localization with noisy distance measurements," *IEEE Transactions on Automation Science and Engineering*, vol. 3, no. 4, pp. 360-371, Oct. 2006.

[8] S. Salari, S. Shahbazpanahi and K. Ozdemir, "Mobility-Aided wireless sensor network localization via semidefinite programming," *IEEE Transactions on Wireless Communication*, vol. 12, no. 12, pp. 5966-5978, Dec. 2013.

[9] K. W. Cheung, H. C. So, W.-K. Ma, and Y. T. Chan, "Received signal strength based mobile positioning via constrained weighted least squares," in *Proceedings of 2003 IEEE International Conference on Acoustics, Speech, and Signal Processing*, Hong Kong, April 2003, pp. 137-140.

[10] I. Hindmarch, P. Thomas, M. Beach and A. Nix, "Movement model enhanced RSS localization," in *Proceedings of 2016 International Conference on Localization and GNSS*, Barcelona, Spain, June 2016, pp. 1-6.

[11] P. Biswas and Y. Ye, "Semidefinite programming for ad hoc wireless sensor network localization," in *Proceedings of 3th International Symposium on Information Processing in Sensor Networks*, Berkeley, April 2004, pp. 46-54.

[12] P. Biswas, T.-C. Liang, K.-C. Toh, Y. Ye, and T.-C. Wang, "Semidefinite programming approaches for sensor network localization with noisy distance measurements," *IEEE Transactions on Automation Science and Engineering*, vol. 3, no. 4, pp. 360-371, October 2006.

[13] S. Tomic, M. Beko, and R. Dinis, "RSS-based localization in wireless sensor networks using convex relaxation: noncooperative and cooperative schemes," *IEEE Transactions on Vehicular Technology*, vol. 64, no. 5, pp. 2037-2050, May 2015.

[14] X. H. Tian, M. Wang, W. X. Li, B. Y. Jiang, D. Xu, X. B Wang and J. Xu, "Improve accuracy of fingerprinting localization with temporal correlation of the RSS," *IEEE Transactions on Mobile Computing*, vol. 17, no. 1, pp. 113-126, January 2018.

[15] R. M. Vaghefi, M. R. Gholami, R. M. Buechrer, and E. G. Ström, "RSS-based sensor localization with unknown transmit power," in *Proceedings of 2011 IEEE International Conference on Acoustics, Speech and Signal Processing*, Prague, Czech Republic, May 2011, pp. 2480-2483.

[16] R. M. Vaghefi, M. R. Gholami, R. M. Buechrer, and E. G. Ström, "Cooperative received signal strength-based sensor localization with unknown transmit powers," *IEEE Transactions on Signal Processing*, vol. 61, no. 6, pp. 1389-1403, March 2013.

[17] B. Song, J. Sun, H. L. Wang, W. D. Xiao, "Convex feasibility problem based geometric approach for device-free localization," in *Proceedings of 2017 International Conference on Information Fusion*, Xi'an, China, July 2017, pp. 1140-1146.

[18] X. Sheng and Y.-H. Hu, "Maximum likelihood multiple-source localization using acoustic energy measurements with wireless sensor networks," *IEEE Transactions on Signal Processing*, vol. 53, no. 1, pp. 44-53, Janurary 2005.

[19] Q. Wang, Z. S. Duan, X. R. Li, "Emission source localization and sensor registration using RSS measurements," in *Proceedings of 2017 International Conference on Information Fusion*, Xi'an, China, July 2017, pp. 43-50.

[20] C. Wang, F. Qi, G. M. Shi, "Convex combination based target localization with noisy angle of arrival measurements," *IEEE Wireless Communiations Letters*, vol. 3, no. 1, pp. 14-17, February 2014.

[21] N. Patwari, A. O. Hero, M. Perkins, N. S. Correal, R. J. O'Dea, "Relative location estimation in wireless sensor networks," *IEEE Transactions on Signal Processing*, vol. 51, no. 8, pp. 2137-2148, August 2003.

[22] S. Boyd and L. Vandenberghe, *Convex Optimization*. Cambridge, UK: Cambridge University Press, 2004.

[23] T. Rappaport, *Wireless Communications Principles and Practice*. Englewood Cliffs, NJ, USA: Prentice-Hall, 1999.